Journal of Pathology
J Pathol March 2021; **253:** 292–303
Published online 11 December 2020 in Wiley Online Library (wileyonlinelibrary.com) DOI: 10.1002/path.5587

ORIGINAL PAPER

Genetic ablation of *FASN* attenuates the invasive potential of prostate cancer driven by *Pten* loss

Débora C Bastos[1,2†], Caroline F Ribeiro[3†], Thomas Ahearn[4], Jéssica Nascimento[1], Hubert Pakula[3], John Clohessy[5], Lorelei Mucci[4], Thomas Roberts[6], Silvio M Zanata[7], Giorgia Zadra[1] and Massimo Loda[1,3,8,9*]

[1] *Department of Oncologic Pathology, Dana-Farber Cancer Institute, Boston, MA, USA*
[2] *Department of Oral Biosciences, University of Campinas, Piracicaba, Brazil*
[3] *Department of Pathology and Laboratory Medicine, Weill Cornell Medicine, NewYork-Presbyterian Hospital, New York, NY, USA*
[4] *Department of Epidemiology, Harvard T.H. Chan School of Public Health, Boston, MA, USA*
[5] *Beth Israel Deaconess Medical Center, Harvard Medical School, Boston, MA, USA*
[6] *Department of Cancer Biology, Dana-Farber Cancer Institute, Boston, MA, USA*
[7] *Departments of Basic Pathology and Cell Biology, Universidade Federal do Paraná, Curitiba, Brazil*
[8] *New York Genome Center, New York, NY, USA*
[9] *The Broad Institute, Cambridge, MA, USA*

**Correspondence to: M Loda, Department of Pathology and Laboratory Medicine, Weill Cornell Medicine, 1300 York Avenue, Room C-302/Box 69, New York, NY 10065, USA. E-mail: mloda@med.cornell.edu*

[†]These authors contributed equally to this work.

Abstract

Loss of the tumor suppressor gene *Pten* in murine prostate recapitulates human carcinogenesis and causes stromal proliferation surrounding murine prostate intraepithelial neoplasia (mPIN), which is reactive to microinvasion. In turn, invasion has been shown to be regulated in part by *de novo* fatty acid synthesis in prostate cancer. We therefore investigated the effects of genetic ablation of *Fasn* on invasive potential in prostate-specific *Pten* knockout mice. Combined genetic ablation of *Fasn* and *Pten* reduced the weight and volume of all the prostate lobes when compared to single knockouts. The stromal reaction to microinvasion and the cell proliferation that typically occurs in *Pten* knockout were largely abolished by *Fasn* knockout. To verify that *Fasn* knockout indeed results in decreased invasive potential, we show that genetic ablation and pharmacologic inhibition of FASN in prostate cancer cells significantly inhibit cellular motility and invasion. Finally, combined loss of PTEN with FASN overexpression was associated with lethality as assessed in 660 prostate cancer patients with 14.2 years of median follow-up. Taken together, these findings show that *de novo* lipogenesis contributes to the aggressive phenotype induced by *Pten* loss in murine prostate and targeting *Fasn* may reduce the invasive potential of prostate cancer driven by *Pten* loss.

Keywords: FASN; GEMM; invasion; prostate cancer; PTEN

Received 19 April 2020; Revised 23 September 2020; Accepted 30 October 2020

No conflicts of interest were declared.

Introduction

Prostate cancer (PCa) is the second most common cancer in men worldwide and is the second leading cause of cancer death in American men (World Health Organization – Globocan, 2016). Deletions and mutations in the tumor suppressor gene phosphatase and tensin homologue (*PTEN*), which encodes the PTEN protein, are among the most frequent alterations found in prostate cancer, particularly in the metastatic setting [1–3]. Loss of *PTEN* expression is found in 17% of primary and 40.7% of metastatic prostate cancer and is associated with worse prognosis and shorter recurrence-free survival [3–9], especially in ERG-fusion negative samples [10,11]. *PTEN* loss of activity due to mutations or deletions results in PIP3 accumulation and activation of the PI3K/AKT pathway [12,13]. In fact, PI3K/AKT is the most frequently activated pathway in human malignant neoplasms, including prostate cancer [1,10,14].

Activation of PI3K/Akt signaling enhances invasive potential by modulating different targets in the cell, which facilitates prostate cancer progression. In human cells, *PTEN* overexpression decreases cell proliferation and migration due to reduced AKT phosphorylation [15]. Markers of invasion such as urokinase-type plasminogen activator (uPA) and matrix metalloproteinase (MMP)-9 are downregulated with *PTEN* expression or PI3K/AKT blockade [16]. In human and murine prostate

cancer cells, increased expression of Cxcl12 and its receptor Cxcr4 follows PI3K/Akt activation, inducing cellular invasion and tumor growth [17]. Bone metastases are enhanced by angiogenesis induced by N-cadherin through PI3K/AKT signaling [18], and by activation of the bone morphogenetic protein (BMP) signaling cascade through the PI3K/AKT–NF-κB axis [19].

Fatty acid synthase (FASN) enzyme is an androgen-regulated gene, responsible for *de novo* synthesis of long-chain fatty acids. Lipid synthesis is essential for new cellular membrane synthesis required during cell division, for the post-translational modification of signaling molecules, as well as for energy storage [20]. FASN facilitates oncogenesis when overexpressed in the mouse [21]. FASN is expressed at low to undetectable levels in normal tissues, except in breast during lactation, in liver, and in proliferative phase endometrium [22]. Also, non-malignant cells typically acquire palmitate from the diet [23] and FASN inhibition minimally affects normal cells, including prostate [24]. On the other hand, elevated levels of FASN were found in prostates of transgenic mice of prostate adenocarcinoma (TRAMP) and its levels increased with age, tumor progression, and metastasis [25]. FASN is overexpressed in human prostate cancer, especially in the metastatic, castration-resistant setting [26–30], and is associated with poor prognosis [29,31]. The lipid biosynthesis process has been associated with invasion and metastasis. Inhibition of acetyl-CoA carboxylase (ACC), another essential enzyme for the biosynthesis of fatty acids, decreases invadopodia formation and the ability of prostate cancer cells, among others, to invade [32]. In addition, *FASN* inhibition with siRNA in LNCaP cells reduces pseudopodia and invadopodia formation, cell adhesion, migration, and invasion [33]. Also, *FASN* inhibition with shRNA mediates actin cytoskeletal remodeling by decreasing the palmitoylation of Rho GTPases and the downstream activation of Cdc2, resulting in reduced prostate cancer cell migration [34]. Finally, *FASN* inhibition negatively regulates cytosolic phospholipase A2 (PLA2G4A) and estradiol 17-beta-dehydrogenase 12 (HSD17B12) in several prostate cancer cell lines. These enzymes, responsible for arachidonic acid and androgen production, respectively, when downregulated cause a decrease of downstream genes such as *RGS2*, *SPAG16*, *VWF*, and *RAP2B*, which are also involved in cellular motility, proliferation, and extracellular matrix interaction [33].

Somatic heterozygous deletion of *Pten* in mice results in prostatic intraepithelial neoplasia (PIN) by 10 months of age, with approximately 100% penetrance but not metastasis [35]. In contrast, prostate-specific homozygous deletion of *Pten* results in PIN, which progresses to invasive carcinoma by 12–29 weeks. Lymph node metastases occur in 45% and lung metastases in 27% of the mice [35]. Overexpression of *FASN* and altered metabolism in prostate cancer cells are associated with inactivation of *PTEN* [28,36,37]; in contrast, *PTEN* expression is inversely correlated with *FASN* expression in prostate cancer [38], while inhibition of *PTEN* leads to the overexpression of *FASN in vitro*. Here, we characterize the role of *FASN* inactivation in modulating the invasive propensity of *PTEN* knockout (KO) in a genetically engineered modified mouse (GEMM) model.

Materials and methods

Mice

Animal studies were performed according to ARRIVE guidelines and approved by the Dana-Farber Cancer Institute (DFCI) Institutional Animal Care and Use Committee (IACUC, Protocol number: 13-014) in accordance with the NIH Guide for the Care and Use of Laboratory Animals; to the state and federal Animal Welfare Acts; and to institutional guidelines [Beth Israel Deaconess Medical Center (BIDMC) and DFCI]. All animals were maintained in an isolated environment in barrier cages. The generation of single and double KO mice for *Fasn* and *Pten* was conducted in three phases: colony establishment (phase I), generation of the experimental breeders (phase II), and generation of experimental cohorts (phase III). Phases I and II were conducted at the Preclinical Murine Pharmacogenetics Core Facility (Department of Medicine, BIDMC) and phase III was conducted at DFCI. Details are provided in the Supplementary materials and methods.

Prostate tissue dissection and processing

At the endpoints (12 or 40 weeks), mice were weighed and euthanized by CO_2 inhalation followed by cervical dislocation. Prostates were collected, weighed, and the anterior prostate (AP), dorso-lateral prostate (DLP), and ventral prostate (VP) lobes were dissected as previously described [39], individually weighed and measured, and immediately fixed in 10% formaldehyde. Prostate tissues were paraffin-embedded for histology and immunohistochemistry.

Immunohistochemistry and Herovici's staining

Immunohistochemical staining of FASN, PTEN, p-Akt, and Ki-67 was performed on the Leica Bond Rx automated immunostainer (Leica Microsystems, Wetzlar, Germany). Details are provided in Supplementary materials and methods. Herovici's collagen staining was performed as recommended by the manufacturer (StatLab, McKinney, TX, USA) and described by Friend [40]. Briefly, following xylene and ethanol washes, slides were incubated with Herovici solution (to stain young collagen and reticulum blue, mature collagen red, and cytoplasm yellow), washed with 1% acetic acid, and incubated with Weigert's hematoxylin. Reactive stroma was calculated only in the prostate lobes of animals where *Fasn* KO occurred in more than 50% of the epithelial cells by measuring the area of stroma normalized by the total area of the lobe using ImageJ software (National Institutes of Health, Bethesda, MD, USA).

Cell culture

The cells used for both migration and invasion assays ($Pten^{+/-}$) were isolated from prostate tissue of mice heterozygous for *Pten* loss. We followed an established protocol for digestion and single cell suspension [41], and cells were cultured in advanced DMEM/F12 medium (aDMEM/F12) supplemented with 10 mM HEPES, penicillin/streptomycin, 0.5 mM GlutaMAX, B27 Supplement (all from Thermo Fisher, Waltham, MA, USA), 1.25 mM *N*-acetyl-L-cysteine (Sigma-Aldrich, St Louis, MO, USA), 10 μM Y27632 (Tocris Bioscience, Bristol, UK), 250 nM A83-01, 50 ng/ml EGF, 500 ng/ml R-spondin 1, 100 ng/ml Noggin (all from PeproTech, Rocky Hill, NJ, USA), and 1 nM dihydrotestosterone (Sigma-Aldrich). Cells were negative for mycoplasma, assessed using a colorimetric MycoAlert mycoplasma detection kit (Lonza, Walkersville, MD, USA).

Wound healing assay and proliferation

$Pten^{+/-}$ cells (8×10^5) were seeded in 24-well plates in medium containing 500 nM IPI-9119 (US Patents 8,546,432 and 9,346,769, developed by Infinity Pharmaceuticals, Cambridge, MA, USA) or vehicle (DMSO). After 20 h, confluent cell monolayers were scraped with a sterile 200-μl pipette tip to create cell-free areas. After three washes with PBS, medium containing the drug or vehicle was replaced and cells were incubated for 24 h. Images were obtained at 0 and 24 h and cell migration was analyzed with ImageJ. To confirm a specific FASN effect on migration, we also transfected $Pten^{+/-}$ cells for 24 h with 50 nM *Fasn* siRNA (#MSS274301 and #MSS236464; ThermoFisher Scientific, Waltham, MA, USA) and control siRNA (#12935300; ThermoFisher) before seeding cells as a confluent monolayer. Following wound formation, cells were imaged at 0 and 24 h (a total of 48 h incubation with siRNA). To exclude interference of proliferation, we concomitantly counted viable cells. Cells were plated as described and after 48 h were trypsinized and counted using the Vi Cell XR analyzer (Beckman Coulter, Fullerton, CA, USA) based on the trypan blue exclusion method.

Boyden chamber assay

$Pten^{+/-}$ cells (8×10^5) were either pretreated for 24 h with 500 nM IPI-9119/DMSO or transfected for 24 h with 50 nM of *Fasn* siRNAs. Basement membrane-coated inserts (CytoSelect™ CBA-110; Cell Biolabs, San Diego, CA, USA) were incubated for 1 h at room temperature with aDMEM/F12 medium. Treated cells were suspended at 10^6 cells/ml in 300 μl of supplemented aDMEM/F12 medium without serum and seeded onto the upper compartment of the inserts, with DMSO/IPI-9119 or 50 nM siRNA. Medium containing 10% fetal bovine serum (500 μl) was added to the lower chamber and cells were allowed to invade for 2 days. Invasion was quantified by staining the fixed invasive cells (4% formaldehyde for 1 h at room temperature) with toluidine blue.

Western blotting

To confirm FASN knockdown with siRNA, we perform a western blot [20] in the same conditions and at the same time points as the functional assays (proliferation, wound healing, and invasion). Forty-eight and 72 h after siRNA incubation, $Pten^{+/-}$ cells were collected and lysed in RIPA buffer with the addition of phosphatase and protease inhibitor cocktail (Sigma-Aldrich and Roche, Basel, Switzerland). Protein quantification was performed using the Bradford protein assay (Bio-Rad, Hercules, CA, USA) and equal amounts of protein were resolved on precast Tris-glycine polyacrylamide gels (Invitrogen). After transfer to nitrocellulose blotting membrane (Sigma), samples were incubated with primary antibodies to FASN (#3180; CST, Danvers, MA, USA) and vinculin (V9131; Sigma-Aldrich).

Study population

We included 660 men diagnosed with prostate cancer who were participants in the Physicians' Health Study (PHS) [42] or Health Professionals Follow-Up Study (HPFS) [43]. The men were diagnosed between 1983 and 2004 and had archival prostate (prostatectomy and TURP) tumor materials for immunohistochemical evaluation. The PHS included two randomized trials investigating aspirin and vitamin supplements in the prevention of cardiovascular disease and cancer among a total of 29,071 male physicians, including 22,071 men aged 40–84 years starting in 1982 and an additional 7,000 men aged ≥50 years starting in 1999, with all receiving annual follow-up questionnaires. The HPFS is an ongoing cohort of 51,529 male health professionals who have been followed with biennial questionnaires since 1986. Incident prostate cancers (ICD-9: 185) were self-reported and confirmed through medical record and pathology report review. Further details have been provided previously [44].

Clinical and follow-up data

We abstracted data on tumor stage, prostate-specific antigen (PSA) level at diagnosis, and treatments from medical records and pathology reports. Standardized histopathologic review by study pathologists of H&E slides of each case provided uniform Gleason grading [45] as well as identification of areas of tumor for tissue microarray construction. Prostate cancer patients were followed up with written questionnaires to collect detailed information regarding treatments and clinical progression. For prostate cancer cases in the HPFS, treating physicians were contacted to collect clinical course information and to confirm development of metastases. For the PHS, self-reported metastasis has been validated to be reported with high accuracy. Cause of death was determined by medical record and death certificate

review. Follow-up for mortality in the cohorts was greater than 98%.

Statistical methods for human data

To evaluate if the association of tumor FASN with clinical outcomes is modified by PTEN status, we dichotomized protein expression of FASN based on the median expression as described by Nguyen *et al* [46] and cross-classified dichotomized FASN and PTEN tumor status. For PTEN, we used the scoring and validation methods described previously [11]. Details are provided in Supplementary materials and methods.

Results

Fasn genetic ablation reduces prostate tumor progression mediated by *Pten* KO

Prostate-specific loss of the tumor suppressor gene *Pten* results in spontaneous malignant lesions. To assess whether tumor progression induced by *Pten* KO is affected by *de novo* fatty acid production, heterozygous *Pten* and *Fasn* KO mice were crossed using a probasin Cre recombinase system and a breeding scheme was implemented as described in the Materials and methods section and supplementary material, Figures S1 and S2. The resulting $Pten^{loxP/loxP}Fasn^{wt/wt}Cre^{pos}$ (P-KO), $Pten^{wt/wt}Fasn^{loxP/loxP}Cre^{pos}$ (F-KO), and $Pten^{loxP/loxP}Fasn^{loxP/loxP}Cre^{pos}$ (F/P-dKO) mice were analyzed at 12 and 40 weeks of age. After recording body weights, the prostate and its individual lobes (AP, DLP, and VP) were weighed, measured, photographed, and dissected (Figure 1A–E and supplementary material, Figure S3A–E). The specific deletion of *Fasn*, confirmed by IHC staining, decreased the weight and volume of the ventral lobes of 12-week-old (Figure 1B,C) and 40-week-old (supplementary material, Figure S3B,C) mice when compared with *Pten* single knockout mice. Similar results were observed for AP at 12 weeks (Figure 1D,E) but not at 40 weeks (supplementary material, Figure S3D,E). Only animals where *Fasn* KO occurred in more than 50% of the epithelial cells (supplementary material, Figure S4) were included in the analysis.

Prostate-specific *Fasn* KO reduces stromal reaction surrounding intraepithelial neoplasia and proliferation in *Pten* KO context

To investigate the reason for the decreased size and weight of prostate lobes in F/P-dKO compared with P-KO mice, histopathological analysis was performed in all prostate lobes and mouse genotypes that had been generated. As control, we confirmed that the prostates from the F-KO group of 12-week-old (Figure 2A) and 40-week-old mice (supplementary material, Figure S5A) were histologically normal and, as expected, positive for PTEN but negative for p-Akt staining. Also, we observed that whereas *Fasn* KO showed a chimeric pattern of inactivation (Figure 2A and supplementary material, Figure S5A), all epithelial cells in *Pten* KO mice exhibiting PIN were FASN-positive (Figure 2A). Histopathological analysis of experimental groups revealed that the areas of PIN and stroma of anterior and ventral prostate lobes in P-KO mice were 41.05% more extensive compared with F/P-dKO mice ($p < 0.0001$).

We next studied the impact of FASN inactivation on the stromal reaction. We observed a dramatic difference in the quantity of reactive stroma when the ventral lobes of the P-KO (Figure 2B) and F/P-dKO groups (Figure 2C) were compared. The stromal areas in the VP and AP of 12-week-old (Figure 2D,E) and the VP of 40-week-old F/P-dKO (Figure 2F,G and supplementary material, Figure S5C) mice were reduced in comparison to P-KO mice (supplementary material, Figure S5B). Importantly, Ki-67 positive staining of epithelial cells in the stroma was reduced by 27.7% and 26.1% in the AP (Figure 3A) and VP (Figure 3B), respectively, in the F/P-dKO group when compared with P-KO. On the other hand, proliferation in the acini was reduced by 6.7% and 7.2% in the AP and VP, respectively, in the F/P-dKO group in comparison with P-KO.

Several areas of microinvasion were identified in the P-KO prostate (Figure 4D,E), while basal layer integrity was preserved in F-KO (Figure 4A,B) and F/P-dKO mice (Figure 4G,H). The Herovici stain (Figure 4C, F,I) demonstrated that the stroma of prostates in the F-KO group (Figure 4C) was not reactive, devoid of *de novo* synthesized collagen (blue fibers), while the intense stromal reaction in the invasive areas of the P-KO group (Figure 4C) is formed by new collagen fibers permeating old and mature collagen fibers (pink). On the other hand, we observed a sparse stroma in the F/P-dKO group, formed by new collagen fibers between tumor islands that are surrounded by old and mature collagen fibers (Figure 4F), reflective of the loss or deceleration of the invasive phenotype.

FASN depletion reduces PCa cell invasiveness

To confirm the negative effect of *Fasn* KO on the ability of prostate cancer cells to migrate and invade, we inhibited *de novo* fatty acid synthesis by genetic and pharmacologic means in $Pten^{+/-}$ prostate cancer cells. The selective FASN inhibitor IPI-9119 [24] reduced both cell migration (Figure 5A, left panel, and 5B) and invasion (Figure 5A, right panel, and 5C) in $Pten^{+/-}$ prostate cancer cells, but not their viability (Figure 5D). Similar results were obtained with FASN knockdown by siRNA (Figure 5E,F), which was confirmed by western blot (Figure 5G).

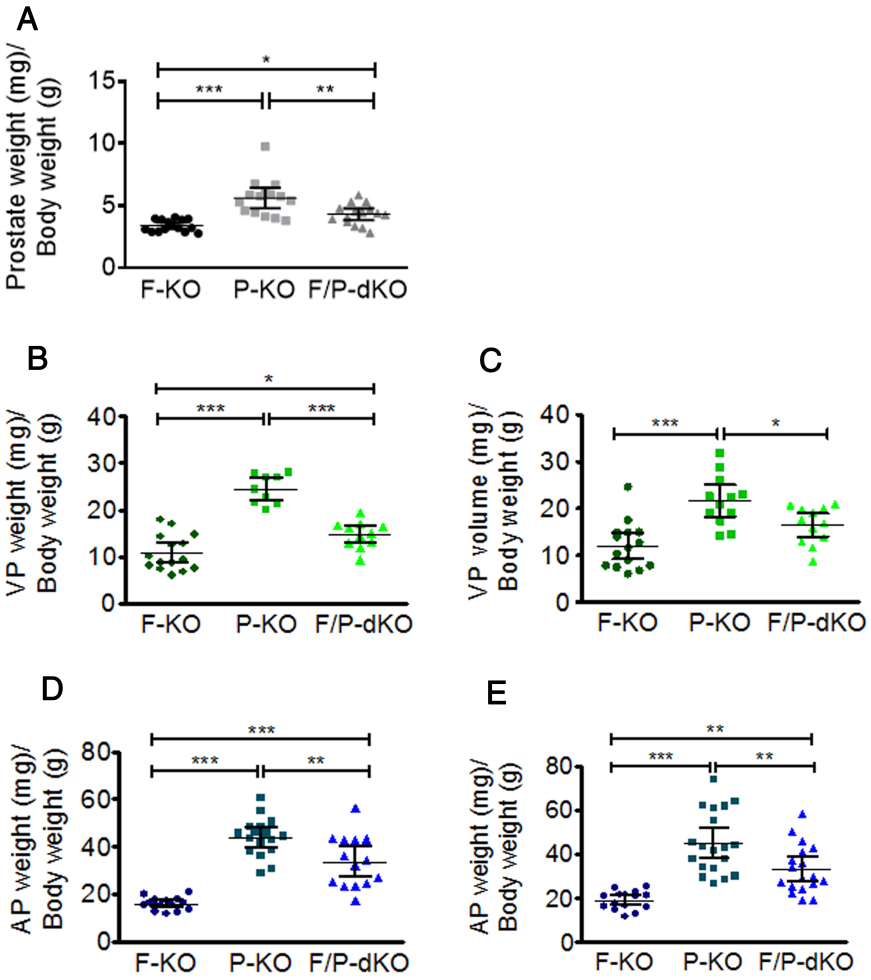

Figure 1. Prostate-specific *Fasn* ablation (F-KO) reduces the volume and/or weight of ventral and anterior prostate cancer induced by *Pten* loss (P-KO) in 12-week-old mice. (A) Whole prostate weight. (B) Ventral prostate weight. (C) Ventral prostate volume. (D) Anterior prostate weight. (E) Anterior prostate volume. Prostate weights were normalized to body weight. *$p < 0.01$, **$p < 0.001$, ***$p < 0.0001$; ANOVA and Tukey's test. Error bars indicate mean ± SD ($n = 15$ mice).

Combined *Pten* loss and FASN overexpression is associated with lethal prostate cancer

We analyzed two prospective cohorts of 660 incident prostate cancer cases diagnosed from 1983 to 2004 from the PHS [42] and HPFS [43]. Tumor FASN expression did not significantly differ by PTEN tumor status ($p = 0.25$). Clinical and demographic characteristics of the cohort by FASN/PTEN status are summarized in Table 1. Men with PTEN loss and high FASN tended to be diagnosed at an older age compared with other groups. Tumors with PTEN loss had higher Gleason grades and more advanced tumor stage irrespective of FASN expression. However, tumors with PTEN loss and high FASN tended to have the most advanced pathologic and clinical TNM stage. Mean body mass index did not differ across the FASN/PTEN groups.

During a mean follow-up of 14.2 years (range 0.11–25.8 years), 70 lethal events occurred. We evaluated and satisfied the proportional hazards assumption by testing the significance of the interaction between cross-classified FASN/PTEN and follow-up time in a model adjusting for age at diagnosis, Gleason grade, clinical TNM, and study cohort (Wald test $p = 0.18$). Table 2 and Figure 6 show the results of cross-classified FASN/PTEN with lethal prostate cancer. In the multivariable models, tumors with PTEN loss and high FASN expression were associated with a higher risk for lethal progression (HR 2.0; 95% CI 1.1–3.9; p interaction = 0.03).

Discussion

The tumor suppressor gene *PTEN* has been extensively associated with prostate cancer development and progression [2–4,6–9]. Metabolic changes also occur during prostate tumorigenesis, including alterations in *de novo* lipogenesis [37,47,48]. Increased levels of FASN are observed in the early phase of prostatic carcinogenesis and its overexpression is associated with poor prognosis, metastasis, and chemoresistance [21,26,28,29,49,50].

Several studies have reported that pharmacological or genetic FASN inhibition results in cell cycle arrest, apoptosis, and reduction of prostate cancer progression in xenograft models [24,47,51,52]. Previous studies in

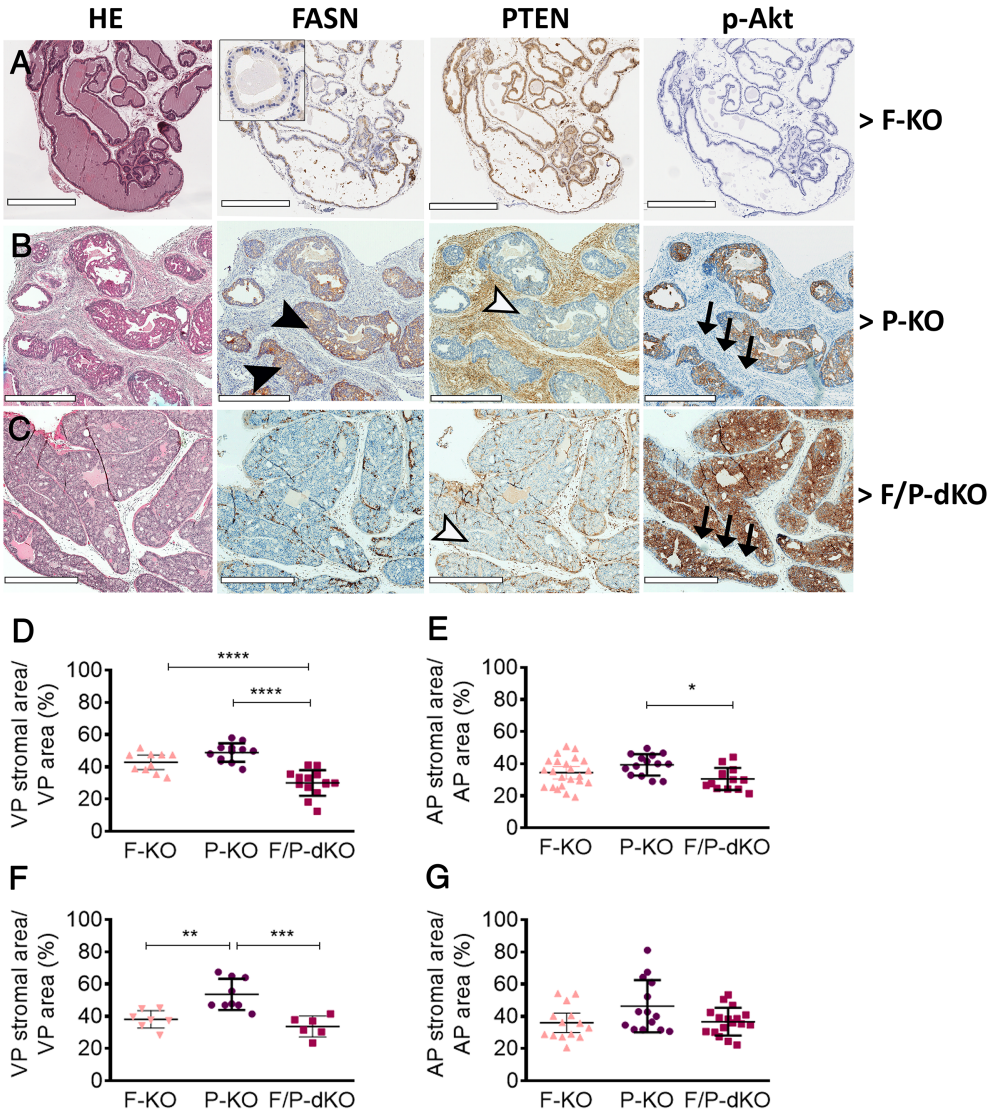

Figure 2. Conditional F-KO affects prostate cancer progression through reduction of stromal and invasive areas in P-KO mice. (A–C) H&E and immunohistochemistry images of the prostates of the indicated mouse strains. Black arrowheads indicate high levels of Fasn; white arrowheads indicate that Pten was deleted in the epithelial cells, but not in the stromal cells of P-KO and F/P-dKO mice; and black arrows indicate lack of p-AKt in stromal cells. (D–E) Image analyses of stromal areas of 12-week old mice and (F-G) 40-week old mice. $^{*}p < 0.05$, $^{**}p < 0.01$, $^{***}p < 0.0001$; unpaired *t*-test. Scale bars = 500 µm (A) and 700 µm (B, C).

prostate cancer were mostly conducted with FASN inhibitors such as C75, orlistat, and triclosan [53–55], whose off-target effects as well as instability and poor solubility/oral availability have limited their use in the clinical setting [56]. However, we recently demonstrated that IPI-9119, a specific and selective inhibitor of FASN, impairs the growth of mCRPC xenografts and human organoids while inducing substantial metabolic reprogramming [24]. In addition, FASN inhibition with TVB-3166 reduced both tubulin palmitoylation and expression, and the combination TVB-3166/paclitaxel decreased prostate (22Rv1) xenograft growth [51]. TVB-2640 (ASC-40, Alcletis and 3V-Bioscience), which shares molecular similarities with TVB-3166, is being used in a phase I clinical trial for patients with solid tumors (NCT02223247) as well as in phase II trials for colon cancer (NCT02980029), KRAS non-small cell lung carcinomas (NCT03808558), astrocytomas (NCT03032484), and ErbB2-positive breast cancer (NCT03179904).

Here, we sought to gain insights into the mechanism responsible for halting progression of castration-resistant prostate tumors with a deficient *Pten* background. First, we observed that prostate-specific *Fasn* deletion is associated with a significant reduction of the stromal area surrounding expanding PIN lesions induced by *Pten* KO. Stromal reaction is likely associated with microinvasion and is typical in P-KO tumors as they advance. Prostate lobes were in fact hardened and enlarged in P-KO mice compared with F/P-KO mice. Inhibition of lipid metabolism has been associated with decreased cellular migration and invasion in several cancer cell lines [57–63]. In addition, the stroma may play a significant role in tumor progression [64] and contributes to gland enlargement and tumor weight. Thus, lobe weighing is useful to indirectly assess tumor

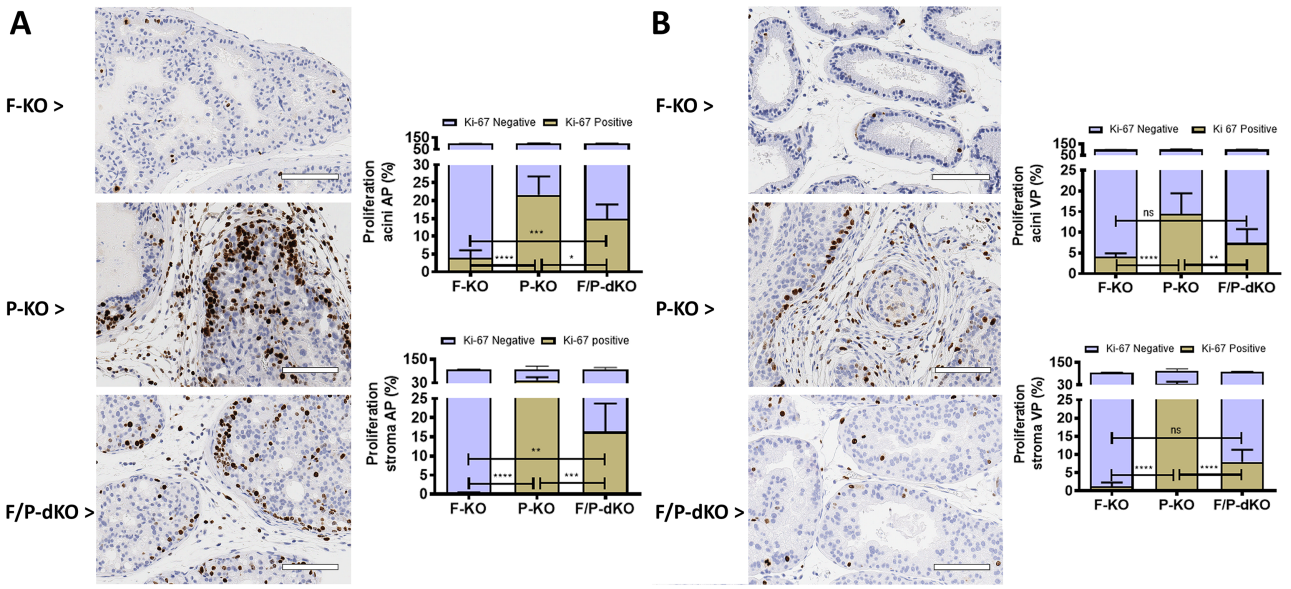

Figure 3. Ki-67-positive epithelial cells are reduced by the *Fasn* genetic ablation in P-KO mice. (A, B) Ki-67 staining and quantitation in 12-week-old mice. (A) Proliferation in the AP. (B) Proliferation in the VP. ns, not significant. $^{*}p < 0.05$, $^{**}p < 0.005$, $^{***}p = 0.0001$, $^{****}p < 0.0001$; ANOVA and Tukey's test. Scale bars = 100 µm.

progression. Acini in P-KO mice are spaced far apart and occupy proportionally less space compared with F/P-KO. Also, proliferation of epithelial cells dispersed in the stroma was reduced in F/P-dKO compared with P-KO. Although the reduction of epithelial cell proliferation in acini was also significant in the F/P-dKO group, this reduction was less pronounced compared with the Ki-67 staining reduction in the stroma.

These results suggest that prostate-specific FASN inactivation affects cancer progression in the early phases of carcinogenesis (12-week-old mice) and that these effects are maintained during tumor progression

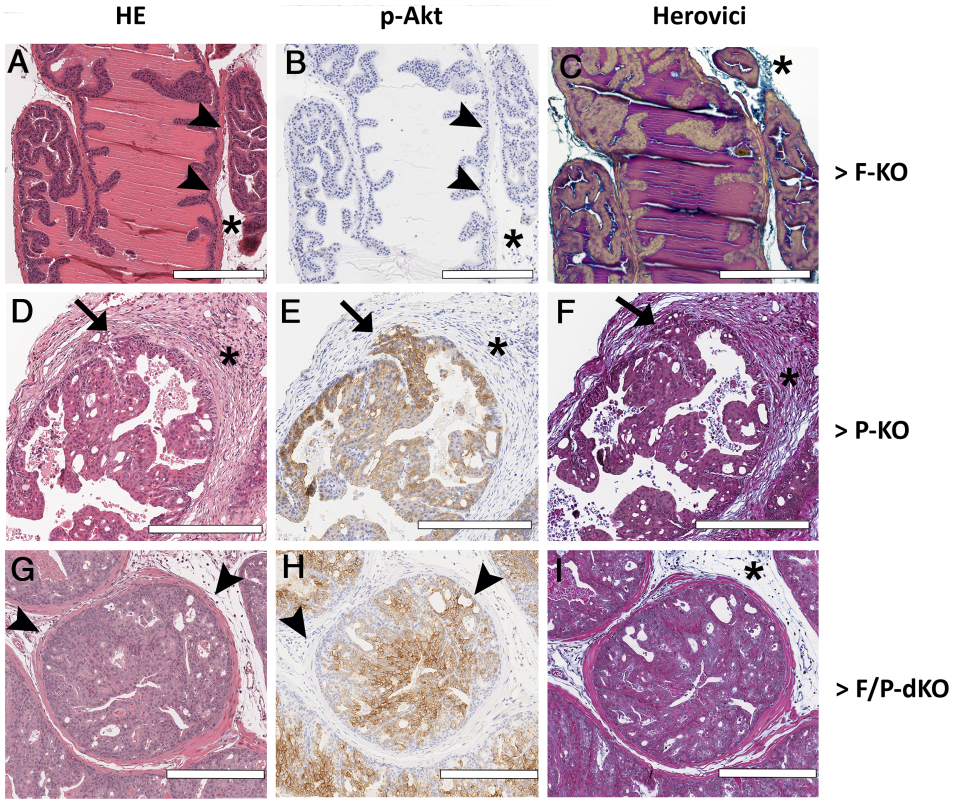

Figure 4. *Fasn* knockout reduced invasive areas in P-KO mice. (A–I) H&E, p-AKT immunohistochemistry and Herovici staining. Asterisk indicates stroma; arrowheads indicate the basal layer; and arrows indicate areas of invasion. Scale bars = 300 µm.

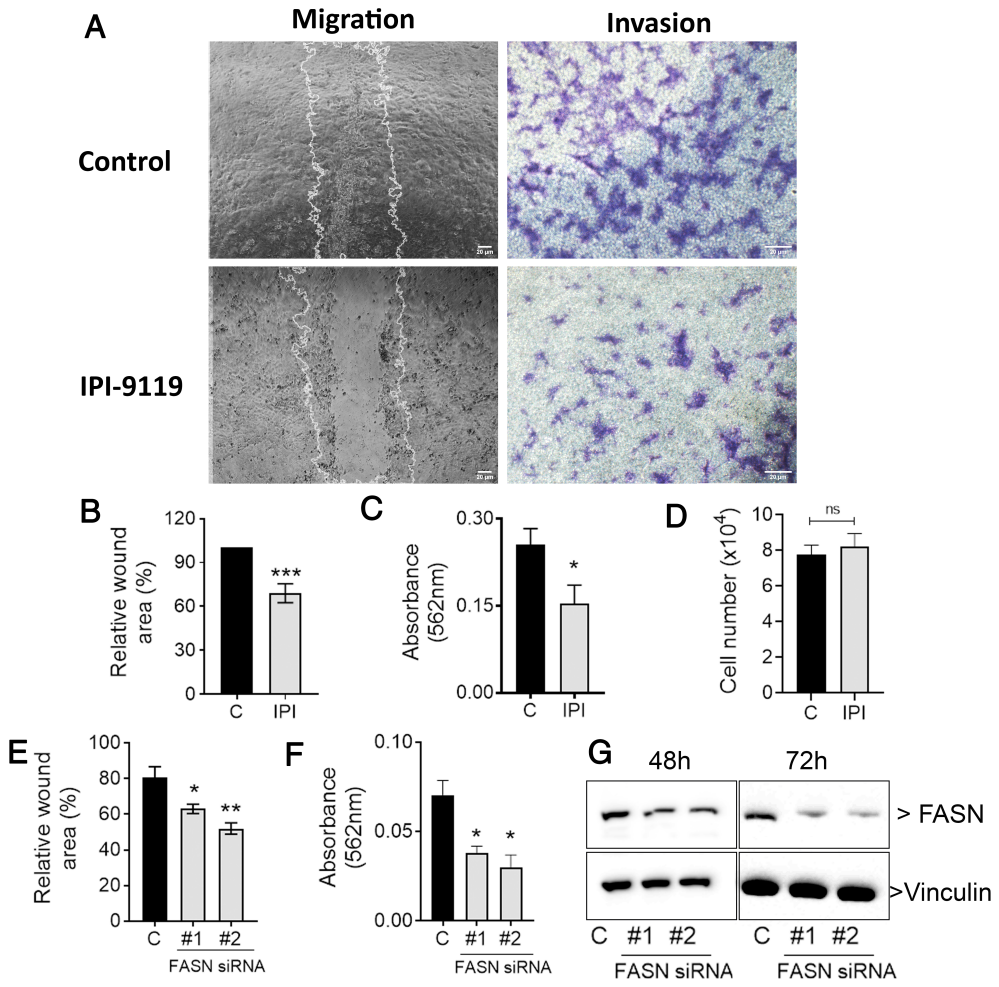

Figure 5. FASN depletion reduces the migration and invasion of murine epithelial PCa PTEN$^{pos/neg}$ cell line. (A) Wound healing (right panel) and invasion through Boyden chambers coated with ECM (left panel) of PTEN$^{+/-}$ prostate cancer cells treated with IPI-119, quantified in B and C. (D) Cell viability for these data. (E, F) Wound healing and invasion of cells treated with *Fasn* siRNAs. (G) Representative immunoblotting for FASN in cells treated for 24 or 48 h with siRNAs. *$p < 0.01$, **$p < 0.001$, ***$p < 0.0001$; ANOVA and Tukey's test. Scale bars = 20 μm.

(40-week-old mice), especially in the VP. In general, effects on weight, volume, and stromal reaction were more pronounced in the VP than in the AP, especially at 40 weeks. We attribute this to the following reasons: the commonly observed accumulation of liquids in 40-week-old mouse AP, which affects the weight, size,

Table 1. Association of cross-classified FASN/PTEN with lethal prostate cancer among men diagnosed with prostate cancer between 1983 and 2004 in the Health Professionals Follow-Up Study and the Physicians' Health Study.

	PTEN intact and FASN low (n = 267)	PTEN intact and FASN high (n = 262)	PTEN loss and FASN low (n = 63)	PTEN loss and FASN high (n = 68)
Mean age at diagnosis, years (SD)	65.9 (6.3)	65.2 (6.4)	65.0 (6.0)	66.8 (6.0)
Mean BMI at diagnosis, kg/m^2 (SD)	25.8 (2.9)	25.7 (4.1)	25.5 (3.0)	25.1 (3.2)
Median PSA at diagnosis (Q1, Q3)*	7.4 (5.3, 11.0)	7.0 (5.0, 10.8)	6.9 (4.8, 10.5)	7.2 (5.0, 12.0)
Gleason grade, *n* (%)				
<6	45 (17)	54 (21)	5 (8)	5 (7)
3 + 4	107 (40)	111 (42)	14 (22)	16 (24)
4 + 3	67 (25)	56 (21)	22 (35)	25 (37)
8+	48 (18)	41 (16)	22 (35)	22 (33)
Pathologic TNM, *n* (%)				
T2 N0/Nx	169 (70)	186 (78)	27 (47)	38 (61)
T3 N0/Nx	69 (29)	48 (20)	29 (50)	17 (27)
T4 N1/M1	4 (2)	6 (3)	2 (3)	7 (11)
Clinical TNM, *n* (%)				
T1/T2	240 (93)	235 (92)	49 (80)	60 (92)
T3 N0/Nx	15 (6)	13 (5)	9 (15)	0 (0)
T4 N1/M1	3 (1)	7 (3)	3 (5)	5 (8)

*Cases with PSA at diagnosis: PTEN intact and FASN low = 221; PTEN intact and FASN high = 231; PTEN low and FASN low = 56; PTEN low and FASN high = 48.

Table 2. Association of cross-classified FASN/PTEN with lethal prostate cancer among men diagnosed with prostate cancer between 1983 and 2004 in the Health Professionals Follow-Up Study and the Physicians' Health Study.

PTEN/FASN expression	*N*	Lethal	HR (95% CI)*	p_{int}†
Any PTEN intact‡/FASN low	267	23	Reference	0.03
Any PTEN intact‡/FASN high	262	24	0.9 (0.5–1.6)	
Complete PTEN loss§/FASN low	63	7	0.6 (0.3–1.5)	
Complete PTEN loss§/FASN high	68	16	2.0 (1.1–3.9)	

*Adjusted for age at diagnosis, cTNM, and Gleason grade.
†*P* value of PTEN and FASN multiplicative interaction based on the Wald test.
‡At least one TMA core with PTEN intact.
§All TMA cores with PTEN loss.

and distance between the acini in the AP, but does not occur in the VP; that the stroma of normal VP is thinner and more delicate than the prominent connective tissue in the stroma of normal AP [65] makes even subtle changes more easily identified in the VP. Consistent with these findings, we have previously shown that knockout of both PI3K mediators (p110 alpha and beta) is required to reverse PIN in the VP, while the loss of p110 beta alone is needed to reverse it in the AP [66]. Thus, the VP is biologically the lobe that requires full PI3K signaling in tumorigenesis and is therefore the more appropriate lobe to assess the differences that we observed. Additionally, it is important to highlight that prostates of F-KO mice were histologically normal, positive for PTEN, and negative for p-Akt staining. Our group has been working with *Fasn* KO mice for many years [67] and we have found no histological differences between prostate, or other organs, in WT and *Fasn* KO mice of the same genetic background at all ages (unpublished data). In addition, it is widely reported that pharmacologic inhibition of FASN minimally affects normal prostate cells [24]. Also, we observed that whereas F-KO showed a chimeric pattern of inactivation in epithelial cells, PIN lesions arising in P-KO are all FASN-positive.

Inhibition of acetyl-CoA carboxylase (ACC) decreases invadopodia formation and the ability of prostate cancer cells to invade [32]. In addition, *FASN* inactivation with siRNA in LNCaP cells reduces pseudopodia and invadopodia formation, cell adhesion, migration and invasion, and *FASN* inhibition negatively regulates PLA2G4A and HSD17B12 in several prostate cancer cell lines [33]. Here, we demonstrated that FASN inhibits tumor progression by reducing the migration and invasion of *Pten* heterozygous prostate cancer cells. Further, *in vitro Fasn* inactivation by shRNA affects the adhesion, migration, and invasion of prostate cancer cell lines via actin cytoskeletal remodeling, achieved by decreasing the palmitoylation of the GTPase RhoU and consequent inactivation of Cdc42 [34].

FASN overexpression was previously associated with *PTEN* inactivation [28]. Bandyopadhyay *et al* [38] demonstrated that inhibition of the tumor suppressor gene *Pten* was inversely correlated with FASN expression in prostate cancer in the clinical setting. In that study, 43 patients with follow-up of 5 years were examined. Inhibition of *PTEN* led to the overexpression of *FASN in vitro* [27]. Here, we validated and extended these data in a cohort of 660 prostate cancer patients with median follow-up of 14.2 years, sufficient to adequately assess outcome [68]. Furthermore, we correlated PTEN and

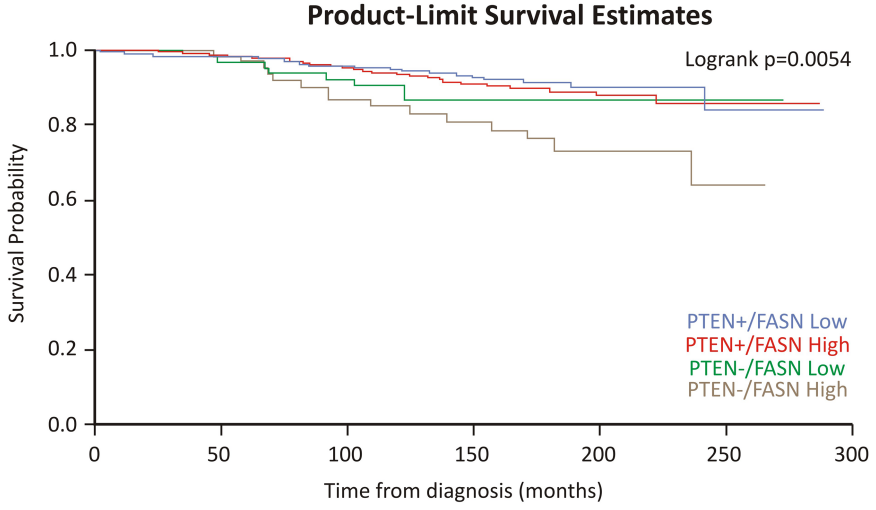

Figure 6. PTEN loss and FASN overexpression are associated with lethal prostate cancer. Kaplan–Meier survival plot for association of the interaction of FASN and PTEN status with lethal prostate cancer among men diagnosed with prostate cancer between 1983 and 2004 within the Health Professionals Follow-Up Study and the Physicians' Health Study.

FASN with clinical characteristics (body mass index, PSA levels, Gleason grade, and pathological and clinical TNM). Interestingly, FASN did not differ by PTEN status, but tumors with PTEN loss and high FASN expression had the most advanced pathologic and clinical TNM stage. Importantly, in the multivariate models, tumors with PTEN loss and high FASN levels were associated with a higher risk for lethal progression. Considering that the new FASN inhibitor TVB-2640 is the first-in-class in clinical trials, the data provide a rationale for utilizing FASN inhibitors in the treatment of prostate cancer, especially those with *Pten* loss.

In conclusion, we demonstrate that *Fasn* genetic ablation reduces invasive potential in the well-established prostate-specific *Pten* knockout mouse model, which arguably reflects one of the most frequent genetic alterations in human prostate cancer [1]. The reduction in stromal reaction induced by invading *Pten*-null cells suggests that *de novo* fatty acid synthesis is required for the invasive and migratory potential of *Pten*-loss prostate cancer cells. Thus, targeting lipid metabolism represents an attractive therapeutic strategy in advanced prostate cancer, especially in tumors harboring *Pten* loss.

Acknowledgements

We thank Dr Rosina Lis (DFCI) for help with immunohistochemical analysis, Dr Marco Bezzi (DFCI) for experimental support, Felipe Paiva (Dental School of Piracicaba, UNICAMP) for slide scanning, Dr Edgard Graner (Dental School of Piracicaba, UNICAMP) for support in the imaging analysis, Dr Xiling Xie (DFCI) for support with statistical analysis, and Sudeepa Syamala (DFCI) for help with maintenance of mouse colonies. This study was supported by the National Institutes of Health (RO1CA131945 to ML, R01CA187918 to TR and ML, P50 CA211024 to ML), Department of Defense (DoD PC160357 and DoD PC180582 to ML), and the Prostate Cancer Foundation. The Health Professionals Follow-Up Study is funded by the National Institutes of Health (U01 CA167552 to LM). Brazilian agencies for research have also supported this work (CNPq grants 551949/2011-2, 309403/2018-9, Fundação Araucária grants 006/2017, PPSUS 058/2017 and PRONEX 116/2018). DCB and CFR were also supported by a scholarship awarded to SMZ (CNPq grant 483610/2012-7).

Author contributions statement

DCB, GZ and ML designed the research study. DCB, CFR, TA, JN, HP and JC conceived and carried out experiments. LM and TR provided human data analysis. DCB, CFR, GZ, SMZ and ML analyzed and interpreted the data. DCB, CFR, GZ and ML wrote and/or reviewed the manuscript. All the authors gave final approval of the submitted and published versions.

References

1. The Cancer Genome Atlas Research Network. The molecular taxonomy of primary prostate cancer. *Cell* 2015; **163:** 1011–1025.
2. Taylor BS, Schultz N, Hieronymus H, *et al*. Integrative genomic profiling of human prostate cancer. *Cancer Cell* 2010; **18:** 11–22.
3. Robinson D, Van Allen EM, Wu YM, *et al*. Integrative clinical genomics of advanced prostate cancer. *Cell* 2015; **161:** 1215–1228.
4. Lotan TL, Gurel B, Sutcliffe S, *et al*. PTEN protein loss by immunostaining: analytic validation and prognostic indicator for a high risk surgical cohort of prostate cancer patients. *Clin Cancer Res* 2011; **17:** 6563–6573.
5. Lotan TL, Carvalho FL, Peskoe SB, *et al*. PTEN loss is associated with upgrading of prostate cancer from biopsy to radical prostatectomy. *Mod Pathol* 2015; **28:** 128–137.
6. Lotan TL, Wei W, Ludkovski O, *et al*. Analytic validation of a clinical-grade PTEN immunohistochemistry assay in prostate cancer by comparison with PTEN FISH. *Mod Pathol* 2016; **29:** 904–914.
7. Lotan TL, Heumann A, Dwertmann Rico S, *et al*. PTEN loss detection in prostate cancer: comparison of PTEN immunohistochemistry and PTEN FISH in a large retrospective prostatectomy cohort. *Oncotarget* 2017; **8:** 65566–65576.
8. Tosoian JJ, Almutairi F, Morais CL, *et al*. Prevalence and prognostic significance of PTEN loss in African-American and European-American men undergoing radical prostatectomy. *Eur Urol* 2017; **71:** 697–700.
9. Jamaspishvili T, Berman DM, Ross AE, *et al*. Clinical implications of PTEN loss in prostate cancer. *Nat Rev Urol* 2018; **15:** 222–234.
10. Krohn A, Diedler T, Burkhardt L, *et al*. Genomic deletion of PTEN is associated with tumor progression and early PSA recurrence in ERG fusion-positive and fusion-negative prostate cancer. *Am J Pathol* 2012; **181:** 401–412.
11. Ahearn TU, Pettersson A, Ebot EM, *et al*. A prospective investigation of PTEN loss and ERG expression in lethal prostate cancer. *J Natl Cancer Inst* 2015; **108:** djv346.
12. Stambolic V, Suzuki A, de la Pompa JL, *et al*. Negative regulation of PKB/Akt-dependent cell survival by the tumor suppressor PTEN. *Cell* 1998; **95:** 29–39.
13. Sun H, Enomoto T, Shroyer KR, *et al*. Clonal analysis and mutations in the PTEN and the K-ras genes in endometrial hyperplasia. *Diagn Mol Pathol* 2002; **11:** 204–211.
14. Elfiky AA, Jiang Z. The PI3 kinase signaling pathway in prostate cancer. *Curr Cancer Drug Targets* 2013; **13:** 157–164.
15. Kimbrough-Allah MN, Millena AC, Khan SA. Differential role of PTEN in transforming growth factor β (TGF-β) effects on proliferation and migration in prostate cancer cells. *Prostate* 2018; **78:** 377–389.
16. Shukla S, Maclennan GT, Hartman DJ, *et al*. Activation of PI3K-Akt signaling pathway promotes prostate cancer cell invasion. *Int J Cancer* 2007; **121:** 1424–1432.
17. Conley-LaComb M, Saliganan A, Kandagatla P, *et al*. PTEN loss mediated Akt activation promotes prostate tumor growth and metastasis via CXCL12/CXCR4 signaling. *Mol Cancer* 2013; **12:** 85.
18. Nalla AK, Estes N, Patel J, *et al*. N-cadherin mediates angiogenesis by regulating monocyte chemoattractant protein-1 expression via PI3K/Akt signaling in prostate cancer cells. *Exp Cell Res* 2011; **317:** 2512–2521.
19. Lien EC, Dibble CC, Toker A. PI3K signaling in cancer: beyond AKT. *Curr Opin Cell Biol* 2017; **45:** 62–71.
20. Zadra G, Loda M. Metabolic vulnerabilities of prostate cancer: diagnostic and therapeutic opportunities. *Cold Spring Harb Perspect Med* 2018; **8:** a030569.
21. Migita T, Ruiz S, Fornari A, *et al*. Fatty acid synthase: a metabolic enzyme and candidate oncogene in prostate cancer. *J Natl Cancer Inst* 2009; **101:** 519–532.

22. Kuhajda FP. Fatty-acid synthase and human cancer: new perspectives on its role in tumor biology. *Nutrition* 2000; **16:** 202–208.
23. Buckley D, Duke G, Heuer TS, *et al*. Fatty acid synthase – modern tumor cell biology insights into a classical oncology target. *Pharmacol Ther* 2017; **177:** 23–31.
24. Zadra G, Ribeiro CF, Chetta P, *et al*. Inhibition of *de novo* lipogenesis targets androgen receptor signaling in castration-resistant prostate cancer. *Proc Natl Acad Sci U S A* 2019; **116:** 631–640.
25. Pflug BR, Pecher SM, Brink AW, *et al*. Increased fatty acid synthase expression and activity during progression of prostate cancer in the TRAMP model. *Prostate* 2003; **57:** 245–254.
26. Epstein JI, Carmichael M, Partin AW. OA-519 (fatty acid synthase) as an independent predictor of pathologic state in adenocarcinoma of the prostate. *Urology* 1995; **45:** 81–86.
27. Swinnen JV, Roskams T, Joniau S, *et al*. Overexpression of fatty acid synthase is an early and common event in the development of prostate cancer. *Int J Cancer* 2002; **98:** 19–22.
28. Van de Sande T, De Schrijver E, Heyns W, *et al*. Role of the phosphatidylinositol 3′-kinase/PTEN/Akt kinase pathway in the overexpression of fatty acid synthase in LNCaP prostate cancer cells. *Cancer Res* 2002; **62:** 642–646.
29. Rossi S, Graner E, Febbo P, *et al*. Fatty acid synthase expression defines distinct molecular signatures in prostate cancer. *Mol Cancer Res* 2003; **1:** 707–715.
30. Shah US, Dhir R, Gollin SM, *et al*. Fatty acid synthase gene overexpression and copy number gain in prostate adenocarcinoma. *Hum Pathol* 2006; **37:** 401–409.
31. Montgomery RB, Mostaghel EA, Vessella R, *et al*. Maintenance of intratumoral androgens in metastatic prostate cancer: a mechanism for castration-resistant tumor growth. *Cancer Res* 2008; **68:** 4447–4454.
32. Scott KEN, Wheeler FB, Davis AL, *et al*. Metabolic regulation of invadopodia and invasion by acetyl-CoA carboxylase 1 and *de novo* lipogenesis. *PLoS One* 2012; **7:** e29761.
33. Yoshii Y, Furukawa T, Oyama N, *et al*. Fatty acid synthase is a key target in multiple essential tumor functions of prostate cancer: uptake of radiolabeled acetate as a predictor of the targeted therapy outcome. *PLoS One* 2013; **8:** e64570.
34. De Piano M, Manuelli V, Zadra G, *et al*. Lipogenic signalling modulates prostate cancer cell adhesion and migration via modification of Rho GTPases. *Oncogene* 2020; **39:** 3666–3679.
35. Wang S, Gao J, Lei Q, *et al*. Prostate-specific deletion of the murine Pten tumor suppressor gene leads to metastatic prostate cancer. *Cancer Cell* 2003; **4:** 209–221.
36. Zhou L, Sheng D, Wang D, *et al*. Identification of cancer-type specific expression patterns for active aldehyde dehydrogenase (ALDH) isoforms in ALDEFLUOR assay. *Cell Biol Toxicol* 2019; **35:** 161–177.
37. Lee YR, Pandolfi P. PTEN mouse models of cancer initiation and progression. *Cold Spring Harb Perspect Med* 2020; **10:** a037283.
38. Bandyopadhyay S, Pai SK, Watabe M, *et al*. FAS expression inversely correlates with PTEN level in prostate cancer and a PI 3-kinase inhibitor synergizes with FAS siRNA to induce apoptosis. *Oncogene* 2005; **24:** 5389–5395.
39. Wang S, Wu J, Suburu J, *et al*. Effect of dietary polyunsaturated fatty acids on castration-resistant Pten-null prostate cancer. *Carcinogenesis* 2012; **33:** 404–412.
40. Friend WG. A polychrome stain for differentiating precollagen from collagen. *Stain Technol* 1963; **38:** 204–206.
41. Lukacs RU, Goldstein AS, Lawson DA, *et al*. Isolation, cultivation and characterization of adult murine prostate stem cells. *Nat Protoc* 2010; **5:** 702–713.
42. Gaziano JM, Glynn RJ, Christen WG, *et al*. Vitamins E and C in the prevention of prostate and total cancer in men: the Physicians' Health Study II randomized controlled trial. *JAMA* 2009; **301:** 52–62.
43. Giovannucci E, Liu Y, Platz EA, *et al*. Risk factors for prostate cancer incidence and progression in the Health Professionals Follow-Up Study. *Int J Cancer* 2007; **121:** 1571–1578.
44. Pettersson A, Lis RT, Meisner A, *et al*. Modification of the association between obesity and lethal prostate cancer by *TMPRSS2:ERG*. *J Natl Cancer Inst* 2013; **105:** 1881–1890.
45. Stark JR, Perner S, Stampfer MJ, *et al*. Gleason score and lethal prostate cancer: does 3 + 4 = 4 + 3? *J Clin Oncol* 2009; **27:** 3459–3464.
46. Nguyen PL, Ma J, Chavarro JE, *et al*. Fatty acid synthase polymorphisms, tumor expression, body mass index, prostate cancer risk, and survival. *J Clin Oncol* 2010; **28:** 3958–3964.
47. Zadra G, Photopoulos C, Loda M. The fat side of prostate cancer. *Biochim Biophys Acta* 2013; **1831:** 1518–1532.
48. Zhou X, Yang X, Sun X, *et al*. Effect of PTEN loss on metabolic reprogramming in prostate cancer cells. *Oncol Lett* 2019; **17:** 2856–2866.
49. Shurbaji MS, Kalbfleisch JH, Thurmond TS. Immunohistochemical detection of a fatty acid synthase (OA-519) as a predictor of progression of prostate cancer. *Hum Pathol* 1996; **27:** 917–921.
50. Wu X, Dong Z, Wang CJ, *et al*. FASN regulates cellular response to genotoxic treatments by increasing PARP-1 expression and DNA repair activity via NF-κB and SP1. *Proc Natl Acad Sci U S A* 2016; **113:** E6965–E6973.
51. Ventura R, Mordec K, Waszczuk J, *et al*. Inhibition of *de novo* palmitate synthesis by fatty acid synthase induces apoptosis in tumor cells by remodeling cell membranes, inhibiting signaling pathways, and reprogramming gene expression. *EBioMedicine* 2015; **2:** 808–824.
52. Heuer TS, Ventura R, Mordec K, *et al*. FASN inhibition and taxane treatment combine to enhance anti-tumor efficacy in diverse xenograft tumor models through disruption of tubulin palmitoylation and microtubule organization and FASN inhibition-mediated effects on oncogenic signaling and gene expression. *EBioMedicine* 2017; **16:** 51–62.
53. Chen H-W, Chang Y-F, Chuang H-Y, *et al*. Targeted therapy with fatty acid synthase inhibitors in a human prostate carcinoma LNCaP/*tk-luc*-bearing animal model. *Prostate Cancer Prostatic Dis* 2012; **15:** 260–264.
54. Kridel SJ, Axelrod F, Rozenkrantz N, *et al*. Orlistat is a novel inhibitor of fatty acid synthase with antitumor activity. *Cancer Res* 2004; **64:** 2070–2075.
55. Sadowski MC, Pouwer RH, Gunter JH, *et al*. The fatty acid synthase inhibitor triclosan: repurposing an anti-microbial agent for targeting prostate cancer. *Oncotarget* 2014; **5:** 9362–9381.
56. Röhrig F, Schulze A. The multifaceted roles of fatty acid synthesis in cancer. *Nat Rev Cancer* 2016; **16:** 732–749.
57. Wang H, Xi Q, Wu G. Fatty acid synthase regulates invasion and metastasis of colorectal cancer via Wnt signaling pathway. *Cancer Med* 2016; **5:** 1599–1606.
58. Gong J, Shen S, Yang Y, *et al*. Inhibition of FASN suppresses migration, invasion and growth in hepatoma carcinoma cells by deregulating the HIF-1α/IGFBP1 pathway. *Int J Oncol* 2017; **50:** 883–892.
59. Zaytseva YY, Rychahou PG, Gulhati P, *et al*. Inhibition of fatty acid synthase attenuates CD44-associated signaling and reduces metastasis in colorectal cancer. *Cancer Res* 2012; **72:** 1504–1517.
60. Bastos DC, Paupert J, Maillard C, *et al*. Effects of fatty acid synthase inhibitors on lymphatic vessels: an *in vitro* and *in vivo* study in a melanoma model. *Lab Invest* 2017; **97:** 194–206.
61. Seguin F, Carvalho MA, Bastos DC, *et al*. The fatty acid synthase inhibitor orlistat reduces experimental metastases and angiogenesis in B16-F10 melanomas. *Br J Cancer* 2012; **107:** 977–987.
62. Agostini M, Almeida LY, Bastos DC, *et al*. The fatty acid synthase inhibitor orlistat reduces the growth and metastasis of orthotopic tongue oral squamous cell carcinomas. *Mol Cancer Ther* 2014; **13:** 585–595.

63. Stoiber K, Nagło O, Pernpeintner C, *et al*. Targeting *de novo* lipogenesis as a novel approach in anti-cancer therapy. *Br J Cancer* 2018; **118:** 43–51.
64. Tyekucheva S, Bowden M, Bango C, *et al*. Stromal and epithelial transcriptional map of initiation progression and metastatic potential of human prostate cancer. *Nat Commun* 2017; **8:** 420.
65. Knoblaugh S, True L. Male reproductive system. In Comparative Anatomy and Histology. A Mouse and Human Atlas *(1st edn), Treuting PM, Dintzis SM (eds)*. Academic Press: Amsterdam, 2012; 285–308.
66. Lee SH, Poulogiannis G, Pyne S, *et al*. A constitutively activated form of the p110β isoform of PI3-kinase induces prostatic intraepithelial neoplasia in mice. *Proc Natl Acad Sci U S A* 2010; **107:** 11002–11007.
67. Chakravarthy MV, Pan Z, Zhu Y, *et al*. "New" hepatic fat activates PPARα to maintain glucose, lipid, and cholesterol homeostasis. *Cell Metab* 2005; **1:** 309–322.
68. Hamdy FC, Donovan JL, Lane JA, *et al*. 10-year outcomes after monitoring, surgery, or radiotherapy for localized prostate cancer. *N Engl J Med* 2016; **375:** 1415–1424.
69. Trotman LC, Niki M, Dotan ZA, *et al*. Pten dose dictates cancer progression in the prostate. *PLoS Biol* 2003; **1:** E59.
70. Wu X, Wu J, Huang J, *et al*. Generation of a prostate epithelial cell-specific Cre transgenic mouse model for tissue-specific gene ablation. *Mech Dev* 2001; **101:** 61–69.
71. Berquin IM, Min Y, Wu R, *et al*. Expression signature of the mouse prostate. *J Biol Chem* 2005; **280:** 36442–36451.
72. Berquin IM, Min Y, Wu R, *et al*. Modulation of prostate cancer genetic risk by omega-3 and omega-6 fatty acids. *J Clin Invest* 2007; **117:** 1866–1875.

References 69–72 are cited only in the supplementary material.

SUPPLEMENTARY MATERIAL ONLINE

Supplementary materials and methods

Figure S1. Breeding scheme for P-KO, F-KO, and F/P-dKO mouse generation

Figure S2. *Pten* and *Fasn* prostate-specific deletion

Figure S3. Prostate weights, volumes and stromal areas at 40 weeks

Figure S4. Discriminating Fasn-positive and -negative regions

Figure S5. Histological and immunohistochemical aspects of 40-week-old prostates

Table S1. Summary of the primers and PCR conditions used